Research Square

Preprints are preliminary reports that have not undergone peer review.
They should not be considered conclusive, used to inform clinical practice,
or referenced by the media as validated information.

Cultivar-Dependent Physiological and Reproductive Responses of Mature Avocado Trees under Mediterranean Weather Extremes: A Three-Year Field Study

Michal Lahack
Northern Agriculture R&D, MIGAL – Galilee Research Institute,
Michael Noy
Agricultural Extension Service, Israel Ministry of Agriculture & Rural Development
Nitzan Szenes
Avocado professional instructor (private)
Lior Rubinovich
liorr@migal.org.il

Northern Agriculture R&D, MIGAL – Galilee Research Institute,

Research Article

Keywords: Abiotic stress, Cultivar variation, Frost injury, Gas exchange, Persea americana, Reproductive resilience

Posted Date: October 29th, 2026

DOI: https://doi.org/10.21203/rs.3.rs-10916675/v1

License: This work is licensed under a Creative Commons Attribution 4.0 International License.
Read Full License

Additional Declarations: No competing interests reported.

Abstract

Background-

Extreme weather events increasingly threaten avocado production, yet it remains unclear whether cultivar-dependent differences in physiological responses are accompanied by differences in reproductive survival and subsequent yield under field conditions. We therefore evaluated the physiological and reproductive responses of mature ‘Hass’, ‘BL122’ (‘BL’), ‘Gem’, and ‘Maluma’ avocado trees during a three-year field study under naturally occurring Mediterranean weather extremes in northern Israel.

Results-

During the study period, the orchard experienced substantial environmental variation, including a severe frost event in February 2025, when air temperature fell to − 3.47°C and remained below 0°C for approximately 10 h, and episodes of extreme summer heat, with a maximum air temperature of 47.2°C. Following the severe frost event, floral bud damage reached 88% in ‘Hass’ and 95% in both ‘BL’ and ‘Maluma’, whereas ‘Gem’ sustained significantly lower damage, with 57% injured buds. Cultivar × season interactions were significant for flowering intensity and all productivity traits. Following the frost, ‘Gem’ showed significantly higher flowering intensity and produced 37.7 kg fruit tree^{-1}, whereas yields of ‘Hass’, ‘BL’, and ‘Maluma’ remained below 2.2 kg tree^{-1}. Physiological responses varied significantly among sampling dates, with significant cultivar × sampling date interactions for CO_2 assimilation, stomatal conductance, Fv/Fm, and CCI. ‘Gem’ maintained relatively high gas-exchange values on several sampling dates, including after the frost event. Fv/Fm reached its lowest values following the frost but recovered to approximately 0.82–0.85 across all cultivars by May 2025, despite pronounced differences in subsequent reproductive performance among cultivars. ‘BL’ frequently showed a higher chlorophyll content index and produced large fruit, but these traits were not accompanied by high post-frost yield.

Conclusions-

Overall, the results reveal substantial cultivar-dependent differences in reproductive resilience following the severe frost event, with ‘Gem’ showing the greatest post-frost flowering intensity and yield among the evaluated cultivars. In contrast, the recovery of physiological indicators did not consistently parallel reproductive recovery across cultivars. These findings highlight the importance of integrating physiological and reproductive responses when evaluating cultivar resilience to extreme weather under field conditions.

1. Background

Avocado is a commercially important evergreen fruit tree cultivated in tropical and subtropical regions worldwide [1]. Despite increasing global demand, avocado production remains highly vulnerable to harsh environmental conditions, particularly extreme heat and cold events, which constrain its geographical expansion and limit stable productivity [2]. Climate change is increasing the exposure of agricultural systems to temperature extremes and greater climatic variability, creating additional challenges for perennial fruit production [3]. Extreme heat events can severely impair avocado growth and survival, and may even lead to tree mortality. Temperature extremes can disrupt key physiological processes in avocado, including carbon assimilation, stomatal regulation, photosystem II performance, and plant water relations [4–6]. The magnitude of these effects depends on stress intensity and duration, as well as on the developmental stage at which exposure occurs [7, 8]. Extreme cold events can be classified into two categories: (i) chilling events, in which temperatures approach but remain above 0°C [9], and (ii) frost events, during which temperatures fall below the freezing point of water [10]. Although chilling events are less severe than frost events, they can still negatively affect avocado physiology. Even in the absence of visible tissue damage, exposure of 'Hass' avocado trees to chilling temperatures was found to reduce maximum CO_2-assimilation rates, light-saturation points, CO_2-saturation points, and quantum yields relative to non-stressed trees. Furthermore, declines in variable-to-maximum chlorophyll fluorescence ratios (Fv/Fm) were reported in 'Hass', 'Reed', and 'Pinkerton' avocado leaves following chilling exposure, indicating chill-induced photoinhibition under winter conditions [11–13]. Frost imposes additional injury through extracellular ice formation, cellular dehydration, membrane disruption, and oxidative stress, and can damage both vegetative and reproductive tissues [14–17]. In avocado, frost injury has been associated with reductions in Fv/Fm, CO_2 assimilation, and stomatal conductance, as well as with damage to foliage, floral buds, flowers, and fruit [18–22].

'Hass', a Guatemalan–Mexican hybrid developed approximately a century ago, remains the dominant avocado cultivar worldwide because of its favorable fruit quality, including creamy texture, rich flavor, and thick peel [23]. Consequently, avocado breeding programs have focused on developing high-quality 'Hass'-like cultivars with improved productivity, fruit characteristics, shelf life, and environmental adaptability and reduced alternate bearing [24, 25]. Among these, 'Maluma', 'Gem', and 'BL122' ('BL') have garnered commercial interest due to their favorable horticultural traits and marketability. The early-bearing 'Maluma', originating from South Africa, is characterized by high productivity and an extended harvest period [26]. 'Gem' and 'BL', both developed at the University of California breeding program, exhibit desirable fruit quality together with advantageous tree architecture, productivity, and fruit-size characteristics [27, 28]. Because these cultivars differ in growth habit, phenology, and reproductive characteristics, they also provide a useful system for testing whether variation among cultivars is associated with contrasting physiological and reproductive responses to environmental stress.

A study of young, non-bearing 'Hass' and 'Hass'-like avocado cultivars showed cultivar-dependent responses to naturally occurring frost and heat events, with 'Gem' exhibiting lower floral bud injury and 'BL' maintaining relatively high chlorophyll content under stressful field conditions [22]. However, it remains unclear whether the cultivar-dependent responses observed in young trees persist after trees begin bearing fruit and, importantly, whether differences in physiological responses are accompanied by

differences in reproductive survival and subsequent productivity. Field-based evidence linking extreme-weather responses to reproductive injury, flowering, and subsequent yield in mature, fruit-bearing 'Hass'-like avocado cultivars is still limited. We hypothesized that cultivars would differ in both their physiological responses to environmental extremes and their capacity to maintain reproductive function following severe frost. Therefore, this study aimed to evaluate the physiological and reproductive responses of mature, fruit-bearing 'Hass'-like avocado cultivars under naturally occurring weather extremes relative to 'Hass'. Specifically, we aimed to determine (i) whether mature, fruit-bearing 'Hass'-like cultivars differ in their physiological responses across contrasting environmental conditions, (ii) whether they differ in floral bud injury, flowering, and productivity following severe frost, and (iii) compare cultivar-specific patterns of physiological response with subsequent reproductive performance. To achieve this, a 3-year field experiment was conducted in northern Israel, in a region characterized by a high frequency of extreme weather events. To our knowledge, this is among the first multi-year field studies to integrate physiological measurements with reproductive injury, flowering, fruit number, and yield in mature, fruit-bearing 'Hass' and 'Hass'-like avocado cultivars under naturally occurring weather extremes. In contrast to previous work in young, non-bearing trees, the present study examines whether cultivar-dependent stress responses persist after trees begin bearing fruit and whether these differences are accompanied by contrasting reproductive performance and yield following severe frost.

2. Methods

2.1 Experimental site and plant material

The study was conducted between January 2023 and March 2026 in a 0.2-ha experimental avocado orchard located at the Northern Agriculture R&D research farm in northeastern Israel (33°09'05"N, 35°37'30"E; 72 m a.s.l.). The orchard soil is characterized by clay texture, comprising 54% clay, 28% silt, and 18% sand. The site was selected because it is frequently exposed to extreme weather conditions. Four avocado cultivars— 'Hass', 'BL', 'Gem', and 'Maluma', all grafted onto the clonal West Indian rootstock 'VC 804'—were evaluated. 'Ettinger' trees were planted as pollinizers, comprising 11% of the plot. Trees were obtained from Dvori Or Nursery (Kfar Haim, Israel) and planted in 2020 in north–south-oriented rows, with a spacing of 4 m between trees within each row and 6 m between rows.

2.2 Experimental design

The trial was arranged as a completely randomized design, with cultivar as the treatment factor (Fig. 1). Each cultivar was represented by 5 replicate plots, each consisting of 3 trees, for a total of 15 trees per cultivar. Trees and leaves sampled within each replicate plot were treated as biological subsamples rather than as independent experimental units. For each response variable, subsample measurements were averaged to obtain a single replicate-level value, and the replicate plot was used as the experimental unit for statistical analysis (n = 5 per cultivar). The same trees were followed across years.

Aerial view of the experimental avocado orchard showing the spatial distribution of the four cultivars. Highlighted tree canopies represent 'Hass' (black), 'BL' (light green), 'Gem' (blue), and 'Maluma' (red).

Each cultivar comprised five replicate plots, with three adjacent trees per replicate. ‘Ettinger’ (yellow) trees were planted as pollinizers, comprising 11% of the plot.

2.3 Meteorological measurements

Meteorological data, including air temperature, relative humidity, precipitation, wind speed, and solar radiation, were obtained from the nearby ‘Ha-Hula’ meteorological station operated by the Israeli Meteorological Service. To complement these records, air temperature and relative humidity were monitored in the orchard during February 2025 using two miniature, waterproof, HOBO data loggers (MX2301A; Onset Corp., Bourne, MA, USA). The loggers were installed 1.5 m above ground level and were shaded by the tree canopy to minimize direct solar exposure. Air temperature and relative humidity were recorded at 10-min intervals.

2.4 Leaf-level light intensity and gas-exchange measurements

Leaf-level photosynthetic photon flux density (PPFD), net CO_2-assimilation rate, and transpiration rate were measured using an LI-6800 portable photosynthesis system equipped with a clear-top 6 cm^2 chamber (LI-COR, Lincoln, NE, USA). During measurements, airflow through the chamber was maintained at approximately 700 $\mu mol\ s^{-1}$, reference CO_2 concentration was set to 415 ppm, and boundary-layer conductance to water vapor was maintained at approximately 3 $mol\ m^{-2}\ s^{-1}$. The chamber temperature and relative humidity were set to ambient. Fully expanded, sun-exposed mature leaves were measured at midday. During the measurements, leaves were maintained in their natural orientation toward the sun while enclosed within the chamber. Stomatal conductance to water vapor (g_s) was calculated by the LI-6800 system. Gas-exchange measurements were conducted on three leaves from the central tree of each replicate. The three leaf measurements from the central tree were averaged to obtain a single value for each replicate plot for statistical analysis. Thus, the replicate plot was treated as the experimental unit, with five independent replicates per treatment (n = 5). The selected leaves were sampled from the southern side of the canopy at a height of approximately 1.5 m above ground level. Leaves chosen for measurements were located four to five nodes from the shoot apex.

2.5 Analysis of chlorophyll a fluorescence and chlorophyll measurements

Leaf chlorophyll *a* fluorescence was measured in the dark at night using a portable FluorPen FP100 fluorometer (Photon Systems Instruments, Drásov, Czech Republic), and Fv/Fm was calculated as previously described [29–31]. Leaf chlorophyll content index (CCI) was determined using a portable chlorophyll meter (MC-100; Apogee Instruments, Logan, UT, USA). For each treatment replicate, measurements were taken from three fully expanded leaves on each of the three trees. The three trees were treated as biological subsamples within the replicate plot. Leaf measurements were first averaged for each tree, and the tree means were then averaged to obtain a single value per replicate. These

replicate-level means were used for statistical analysis. Thus, the replicate plot was the experimental unit, with five independent replicates per treatment (n = 5).

2.6 Flowering intensity estimation

Flowering intensity was evaluated during peak bloom in April 2023, 2024, and 2025, following previously described methods [18, 32]. Two independent evaluators scored each tree separately on a scale of 0 to 5, where 0 indicated no visible flowering, and 5 indicated maximal flowering intensity. Assessments were performed on three trees per replicate. The scores assigned by the two evaluators were first averaged for each tree, and the resulting tree-level means were then averaged across the three trees to obtain one value per replicate. Replicate means were used for statistical analysis (n = 5). The replicate plot was considered the experimental unit. Flowering intensity data from April 2023 were previously reported in Lahack et al. (2025) and are included here solely as the baseline season within the present three-year analysis, enabling evaluation of cultivar-specific flowering patterns in relation to subsequent productivity across seasons.

2.7 Tree yield, fruit number and average fruit weight

During the 3-year experiment, fruits were manually harvested from the experimental trees. Table 1 shows the picking date for the different cultivars. For each replicate, fruit yield was quantified on an individual-tree basis by weighing the total harvested fruit per tree. The total number of harvested fruit was also recorded for each tree. Mean fruit weight (g) was calculated by dividing the total fruit mass by the number of harvested fruit from the corresponding tree. Data were collected from three trees per replicate. Tree-level data were averaged to obtain one value per replicate, and replicate means were used for statistical analysis (n = 5). The replicate plot was considered the experimental unit.

Table 1
Picking dates for the different cultivars during the 3 years of the experiment

Season	**2023–2024**	**2024–2025**	**2025–2026**
Cultivar			
Hass	17 Jan 24	22 Jan 25	20 Jan 26
BL	15 Feb 24	19 Feb 25	4 Mar 26
Gem	15 Feb 24	4 Dec 24	8 Dec 25
Maluma	13 Nov 23	29 Oct 24	9 Nov 25

2.8 Observations of foliage and floral bud damage

Foliage and floral bud damage were evaluated in early March 2025, following the major frost event in February 2025. Floral bud injury was assessed on swollen buds at BBCH stage 511 according to the extended BBCH scale for avocado [1]. Buds were sectioned transversely and visually inspected for

internal browning. Floral buds were classified as damaged when frost-induced browning affected more than 25% of the cross-sectional tissue area. For each replicate plot, 10 buds were assessed on each of three trees, which served as biological subsamples within the replicate plot. Bud-level observations were first averaged for each tree, and tree means were then averaged to obtain a single value per replicate. Statistical analyses were performed using replicate-level means, with the replicate plot considered the experimental unit (n = 5). Visible frost damage to the foliage was assessed using an independent evaluation procedure. Two independent evaluators scored each tree on a scale of 0 to 5, where 0 indicated no visible injury (fully green and healthy foliage) and 5 indicated severe frost damage characterized by extensive leaf browning [18]. Assessments were obtained from three trees per replicate. The scores assigned by the two evaluators were first averaged for each tree, and the resulting tree-level means were then averaged across the three trees within each replicate. Replicate means were used for statistical analysis (n = 5).

2.9 Statistical analysis

Variables measured repeatedly in the same replicate plots were analyzed using linear mixed models. For flowering and productivity variables, cultivar, season, and their interaction were included as fixed effects. For CO_2 assimilation, stomatal conductance, Fv/Fm, and CCI, cultivar, sampling date, and their interaction were included as fixed effects. In all models, the replicate plot was specified as the repeated-measures subject. The covariance structure was selected separately for each response variable based on the corrected Akaike information criterion (AICc), model convergence, and examination of residual diagnostics. The significance of fixed effects was evaluated using Type III F-tests. Following a significant interaction, cultivar least-squares means were compared within each sampling date or season using Tukey-adjusted comparisons. Single-time-point foliage damage scores were analyzed using one-way analysis of variance (ANOVA) followed by Tukey's HSD test. Floral bud damage was analyzed using a binomial generalized linear mixed model (GLMM) with a logit link, with cultivar included as a fixed effect and replicate plot as a random effect. The response was specified as the number of damaged buds relative to the total number of buds assessed for each tree. Pairwise comparisons among cultivars were adjusted using the Tukey–Kramer method. Statistical analyses were performed using JMP software version 18.2.2 (SAS Institute, Cary, NC, USA). Principal component analysis (PCA) was conducted using GraphPad Prism version 11.0.2 software (GraphPad Software, LLC) as an exploratory analysis of multivariate relationships among physiological and productivity traits across avocado cultivars. Annual mean values were calculated separately for each replicate plot and season. To account for cultivar-specific phenological and production cycles, seasonal windows were defined for each cultivar based on its harvest dates each season (Table 1). The variables included in the PCA were CO_2-assimilation rate, g_s, CCI, Fv/Fm, yield, fruit number, and mean fruit weight. Biplots were generated to visualize cultivar clustering patterns and the contribution of individual variables to principal component separation.

2.10 Use of large language model

ChatGPT (OpenAI) was used during manuscript preparation to assist with language editing and improve clarity and organization. All scientific content, statistical analyses, interpretation of the results, and final

wording were reviewed and approved by the authors.

3. Results

3.1 Environmental conditions and extreme weather events in the experimental plot

Substantial seasonal variation in meteorological conditions was recorded throughout the experimental period (January 2023–March 2026; Fig. 2). Air temperatures followed a clear annual cycle, with low winter temperatures and high summer temperatures (Fig. 2, A). During the study period, minimum air temperatures occasionally dropped below 0°C, with the lowest at approximately − 3.5°C during the severe frost event in February 2025. Maximum air temperatures exceeded 40°C during the summer months (April to September), peaking at 47.2°C in August 2025. Relative humidity exhibited considerable temporal variability, with minimum values frequently dropping below 20% during the summer and maximum values remaining close to saturation during much of the experimental period (Fig. 2, B). Precipitation events were sporadic and occurred primarily during the winter months, with several intense rainfall events exceeding 40–50 mm day^{-1} (Fig. 2, C). Maximum wind speed fluctuated substantially throughout the study period, with peak values occasionally exceeding 25 m s^{-1}, particularly during the winter and transitional seasons (Fig. 2, D). Maximum solar radiation also followed a seasonal pattern, with the highest values recorded during spring and summer (Fig. 2, E). Overall, the experimental orchard experienced substantial environmental fluctuations, including a severe frost event and episodes of exceptionally high summer air temperature.

3.2 Cultivar-dependent injury following the February 2025 frost

A severe frost event occurred in the experimental orchard during the night of 24/25 Feb 2025, when the minimum air temperature dropped to − 3.47°C. Air temperature remained below 0°C from 2110 h on 24 February until 0740 h on 25 February, resulting in approximately 10 h of freezing conditions (Fig. 3, A). Following the frost event, damage was detected in both foliage and floral buds. Foliage damage was most severe in ‘Maluma’, reaching 3.5 on a 0–5 scale and significantly exceeding the damage observed in the other cultivars (Fig. 3, B). Floral bud injury was also extensive and differed significantly among cultivars, ranging from 88% in ‘Hass’ to 95% in both ‘Maluma’ and ‘BL’ (Fig. 3, C). In contrast, ‘Gem’ exhibited significantly lower floral bud damage than all other cultivars (57%). Representative images of frost-damaged trees recorded in March 2025 are presented in Fig. 3, D.

3.3 Flowering intensity and reproductive parameters of the different cultivars

Linear mixed-model analysis revealed significant effects of cultivar, season, and cultivar × season interaction on flowering intensity, yield, fruit number, and mean fruit weight (Table 2). The significant interactions indicate that cultivar differences varied among seasons. Therefore, cultivar means were subsequently compared separately within each season.

Table 2
Significance of the fixed effects of cultivar, season, and their interaction on flowering and productivity traits. Results are based on Type III F-tests of fixed effects from the final linear mixed model selected for each response variable. Asterisks indicate significance at * $p < 0.05$, ** $p < 0.01$, and *** $p < 0.001$

Cultivar	Flowering	Yield	Fruit number	Mean fruit weight
	**	**	*	***
Season	***	***	***	***
Cultivar X season	*	***	***	*

In April 2023, flowering was generally high across all cultivars. ‘Maluma’ and ‘Gem’ exhibited the highest flowering intensities, both significantly greater than that of ‘BL’ (Fig. 4, A). However, in ‘Maluma’, despite the high flowering intensity, fruit yield was significantly lower than in the other cultivars, reaching only 2.3 kg tree^{-1} (Fig. 4, B). In contrast, fruit yield in ‘Hass’, ‘BL’, and ‘Gem’ reached 22.5, 38.3, and 23.1 kg tree^{-1}, respectively. The highest fruit number per tree was recorded in ‘Hass’ and ‘BL’, both significantly greater than in ‘Maluma’ (Fig. 4, C). Mean fruit weight was highest in ‘BL’ and ‘Gem’ (237 and 256 g, respectively), significantly exceeding those of ‘Hass’ and ‘Maluma’, which averaged 174 and 194 g, respectively (Fig. 4, D). In April 2024, high flowering intensity was observed in ‘Hass’, ‘Gem’, and ‘Maluma’ (Fig. 4, E), whereas ‘BL’ showed only moderate flowering (2.5 out of 5), significantly lower than the other cultivars. During the corresponding growing season, fruit yield was highest in ‘Hass’, reaching 66.3 kg tree^{-1}, significantly greater than that of ‘Maluma’, which produced only 31.4 kg tree^{-1} (Fig. 4, F). Fruit yield in ‘BL’ and ‘Gem’ reached 39.0 and 52.3 kg tree^{-1}, respectively. Consistent with these results, ‘Hass’ exhibited the highest fruit number per tree (453), whereas fruit number was significantly lower in ‘BL’, ‘Gem’, and ‘Maluma’, with 202, 251, and 211 fruits tree^{-1}, respectively (Fig. 4, G). Similar to the previous season, mean fruit weight was highest for ‘BL’ and ‘Gem’ (229 and 210 g, respectively), significantly greater than those for ‘Hass’ and ‘Maluma’, which averaged 147 and 153 g, respectively (Fig. 4, H). Following the severe frost event of February 2025, flowering intensity in April 2025 was low in all cultivars (Fig. 4, I). Flowering intensity remained below 0.4 in ‘Hass’, ‘BL’, and ‘Maluma’, whereas ‘Gem’ exhibited significantly higher flowering intensity, although values were still relatively low (0.8 out of 5). Correspondingly, fruit yield in ‘Hass’, ‘BL’, and ‘Maluma’ remained below 2.2 kg tree^{-1} (Fig. 4, J). In contrast, ‘Gem’ maintained a significantly higher yield of 37.7 kg tree^{-1}, accompanied by a significantly greater number of fruit per tree compared to all other cultivars (Fig. 4, K). Mean fruit weight was highest for ‘BL’ (304 g), significantly greater than for ‘Maluma’ (216 g; Fig. 4, L). Mean fruit weight for ‘Hass’ and ‘Gem’ was intermediate, averaging 236 and 230 g fruit^{-1}, respectively.

Flowering intensity was assessed and scored in (A) April 2023, (E) April 2024, and (I) April 2025 on a scale of 0–5, with 0 representing no apparent flowering and 5, maximum bloom. (B, F, J) Fruit yield and (C, G, K) number of fruits per tree were determined on the commercial harvest date of each cultivar in the growing seasons of 2023–2024 (B, C), 2024–2025 (F, G), and 2025–2026 (J, K). (D, H, L) Mean fruit weight for the three respective seasons was calculated for the same harvest period by dividing the total fruit weight by the number of fruits on each tree. Values are means ± SE of five replicate plots (n = 5, three trees per replicate). Different letters above a column indicate significant differences within each growing season (Tukey-adjusted comparisons, $P < 0.05$).

3.4 Leaf-level light intensity and gas-exchange parameters in the different cultivars

Leaf-level PPFD was generally similar among cultivars across measurement dates (Supplementary Fig. 1). Linear mixed-model analysis showed significant effects of sampling date and cultivar × sampling date interaction for CO_2 assimilation, stomatal conductance, Fv/Fm, and CCI (Table 3). A significant overall cultivar effect was detected for CO_2 assimilation rate and stomatal conductance, but not for Fv/Fm or CCI. Because the cultivar × sampling date interactions were significant, cultivar differences were further examined separately at each sampling date.

Table 3
Significance of the fixed effects of cultivar, sampling date, and their interaction on physiological traits. Results are based on Type III F-tests from the selected linear mixed models. Asterisks indicate significance at * $p < 0.05$, ** $p < 0.01$, and *** $p < 0.001$; "ns" denotes non-significant. A, net CO_2 assimilation rate; g_s, stomatal conductance; Fv/Fm, maximum quantum yield of photosystem II; CCI, chlorophyll content index

Cultivar	A	g_s	Fv/Fm	CCI
	*	*	ns	ns
Sampling date	***	***	***	***
Cultivar X Sampling date	**	***	***	***

Net CO_2-assimilation rate and g□ varied substantially throughout the experimental period and varied significantly among sampling dates (Fig. 5). In all cultivars, both parameters declined during the cold winters, with particularly low values recorded on 11 Mar and 16 Apr 2025 following the severe frost event of February 2025. A general reduction in both parameters was also observed during the hot summer months of 2024. 'Gem' maintained relatively high CO_2-assimilation rates on several sampling dates, although cultivar differences were not consistent throughout the experimental period (Fig. 5, A). In January 2024, the CO_2-assimilation rate was significantly greater in 'BL' than in 'Maluma'. In May 2024, the CO_2-assimilation rate was significantly lower in 'Maluma' than in all other cultivars. Following the severe frost event of winter 2025, 'Gem' exhibited significantly higher CO_2-assimilation rates than 'BL' in

April 2025. General g_s patterns were similar to those of the CO_2-assimilation rate, with relatively high values in ‘Gem’ on several sampling dates (Fig. 5, B). In January 2024, g values were significantly greater in ‘BL’ than in ‘Maluma’. In June 2024, g values were significantly greater in ‘Gem’ than in ‘Hass’ and ‘BL’. In September 2024, g values were significantly greater in ‘Gem’ and ‘Maluma’ than in ‘Hass’. In October 2024, g values were significantly greater in ‘Gem’ and ‘Maluma’ than in ‘BL’. In April 2025, following the severe frost event of winter 2025, g values were significantly greater in ‘Gem’ than in ‘BL’ and ‘Maluma’. Across the study period, ‘Gem’ frequently maintained relatively high gas-exchange values, although the magnitude and significance of cultivar differences varied among sampling dates, whereas ‘Hass’ showed lower CO_2 assimilation or g_s than other cultivars on several sampling dates.

The LI-COR system was used to measure and calculate (A) net CO_2-assimilation rate (defined as A) and (B) stomatal conductance to water vapor (g_s). Parameters were measured in the orchard periodically at mid-day from January 2024 to December 2025. Values are means ± SE of five replicate plots (n = 5; one tree per replicate; three different leaves were measured from each tree). Different letters indicate significant differences on the specified date (Tukey-adjusted comparisons, $P < 0.05$). Dates are given as day.month.year.

3.5 Maximum quantum yield (Fv/Fm) and chlorophyll content in the different cultivars

Fv/Fm varied over time, with the most pronounced reductions observed during the winter and following the severe frost event of February 2025 (Fig. 6, A). Fv/Fm had already declined during the winter before the frost event, but a substantially greater reduction was observed at the first post-frost measurement in February 2025. Following the frost event, Fv/Fm declined markedly in all cultivars, reaching minimum values in February 2025. Fv/Fm values subsequently increased in all cultivars, with cultivar differences observed during the recovery period. In April 2025, ‘Gem’ showed the highest Fv/Fm values, significantly higher than ‘BL’ and ‘Hass’. By May 2025, Fv/Fm values in all cultivars had recovered to approximately 0.82–0.85 and remained relatively stable thereafter. Significant differences in Fv/Fm were also observed in April–July 2024; however, Fv/Fm values in all cultivars remained above 0.8 during these periods.

CCI also showed temporal and cultivar-dependent variation (Fig. 6, B). The cultivar × sampling date interaction was significant, whereas the overall cultivar effect was not significant (Table 3), indicating that cultivar differences in CCI were date-dependent rather than consistent throughout the study. ‘BL’ exhibited relatively high CCI values on numerous individual sampling dates. Seasonal declines in CCI were observed during May 2024 and 2025. On numerous individual sampling dates, ‘BL’ exhibited significantly higher CCI values than one or more of the other cultivars, although the specific cultivar contrasts varied among dates. In contrast, ‘Gem’ tended to have lower CCI values during the second half of 2025.

Chlorophyll *a* fluorescence was recorded after dark adaptation to calculate Fv/Fm. Parameters were measured in the orchard periodically from January 2024 to December 2025. Fv/Fm was measured in the

dark at night. Values are means ± SE of five replicate plots (n = 5, three trees per replicate; three different leaves were measured from each tree). Different letters indicate significant differences on the specified date (Tukey-adjusted comparisons, $P < 0.05$). Dates are given as day.month.year.

3.6 Principal component analysis (PCA)

The first two axes of the PCA (PC1 and PC2) accounted for 71% of the total variance observed in the dataset (Supplementary Fig. 2). The loading vectors indicated a strong positive association between CO_2-assimilation rate and g_s, as these variables were closely aligned. Yield and fruit number were also strongly associated, loading in a similar direction. In contrast, fruit weight loaded in the opposite direction to yield and fruit number, indicating an inverse association between mean fruit weight and crop-load variables in the multivariate ordination. Chlorophyll content index (CCI) was positively associated with fruit weight, whereas Fv/Fm showed relatively weak loadings on PC1 and PC2 and was positioned near the origin.

In the PCA biplot, replicate-season observations showed cultivar-related patterns in their multivariate distribution. ‘BL’ samples were primarily distributed in the positive region of PC1 and PC2, corresponding to higher gas-exchange activity, chlorophyll content, and fruit weight. ‘Hass’ samples were generally located in the negative region of PC2 and were associated with higher yield and fruit number. ‘Maluma’ observations were more often located in the positive region of PC1 and the negative region of PC2, a region associated with relatively low reproductive output and gas-exchange activity. ‘Gem’ occupied an intermediate position between the other cultivars, reflecting an intermediate multivariate position rather than clear dominance for any single trait group.

4. Discussion

The present study evaluated the physiological and reproductive responses of mature, fruit-bearing ‘Hass’ and ‘Hass’-like avocado cultivars during three years of naturally occurring Mediterranean weather extremes. Three main patterns emerged. First, following the February 2025 frost, pronounced cultivar-dependent reproductive injury was observed, with ‘Gem’ sustaining substantially less floral bud damage than ‘Hass’, ‘BL’, and ‘Maluma’ (Fig. 3). Second, cultivar differences in physiological traits were strongly dependent on sampling date, as indicated by significant cultivar × sampling date interactions. Third, recovery of leaf-level physiological indicators did not necessarily parallel reproductive recovery: Fv/Fm returned to approximately 0.82–0.85 in all cultivars by May 2025 (Fig. 6), whereas subsequent flowering and yield remained strongly differentiated among cultivars (Fig. 4). The lower floral bud injury observed in ‘Gem’ is consistent with previous observations in young trees [22], indicating that a similar cultivar pattern was observed at both young and mature developmental stages, although cultivar-specific differences in floral bud phenology at the time of frost cannot be excluded.

The reproductive response following the frost provides the clearest evidence of cultivar-dependent resilience in the present study. In April 2025, following the February frost event, flowering intensity was low across all cultivars, but ‘Gem’ showed significantly higher flowering intensity than the other cultivars

(Fig. 4). This response was reflected in yield: whereas ‘Hass’, ‘BL’, and ‘Maluma’ produced less than 2.2 kg tree^{-1}, ‘Gem’ produced 37.7 kg tree^{-1} (Fig. 4). The correspondence between lower floral bud injury and greater subsequent flowering in ‘Gem’ suggests that reduced reproductive injury may have contributed to its comparatively high yield following the frost. In avocado, flowering and fruit set are highly sensitive to environmental stress, and frost injury to floral buds can strongly reduce productivity [18]. Therefore, the lower floral bud injury and greater subsequent flowering observed in ‘Gem’ may provide an important advantage in frost-prone regions. The mechanisms underlying this response were not examined in the present study and should be investigated in future work to clarify the physiological and molecular basis of this cultivar’s reproductive response to frost. Potential mechanisms for future investigation include cultivar differences in freezing-induced dehydration and cellular injury, oxidative stress responses, and antioxidant capacity [19, 33, 34]. However, post-frost yield may also have been influenced by previous-season crop load and cultivar-specific alternate-bearing patterns. ‘Hass’, in particular, carried the highest crop in the season preceding the frost. Although the extensive floral bud injury and near-absence of flowering are consistent with frost being a major contributor to the subsequent yield loss, the present study cannot fully separate frost effects from carry-over effects of previous crop load. From a commercial perspective, it should be noted that the value of a cultivar cannot be assessed solely by its total yield. Larger fruit size, harvest timing, market preferences, and price structure may offset lower fruit number in some production systems. ‘BL’ and ‘Gem’ may therefore provide economic advantages in markets that reward larger fruit, whereas ‘Hass’ may remain advantageous in years without severe climatic stress because of its high crop load.

Gas-exchange measurements revealed significant cultivar × sampling date interactions for both CO_2 assimilation and g_s, indicating that cultivar differences were strongly dependent on sampling date rather than being consistent across seasons. In all cultivars, CO_2 assimilation and g_s declined during the winter and reached particularly low values following the severe frost event (Fig. 5). This pattern is consistent with previous studies showing that cold and frost stress reduce photosynthetic activity and g_s in both field-grown and potted plants [20, 22, 33]. Similar winter-related declines in physiological performance have been reported in other fruit crops, including banana [35], indicating that low temperatures can impose broad constraints on carbon assimilation and photosynthetic function. On several sampling dates, ‘Gem’ maintained relatively high CO_2 assimilation and g compared with some of the other cultivars, including during the post-frost period (Fig. 5). These date-specific differences are consistent with ‘Gem’ maintaining relatively high leaf-level carbon assimilation and stomatal conductance under some stressful field conditions, including following the frost event; however, they do not demonstrate consistently greater physiological stress tolerance across the study period. This pattern is also consistent with previous observations of relatively high gas-exchange performance in young ‘Gem’ trees compared **to** ‘Hass’ and ‘Maluma’ under cold field conditions [22].

The reduction in Fv/Fm following the frost event (Fig. 6) provides evidence of a transient impairment of maximum photosystem II photochemical efficiency. Fv/Fm had already declined during the preceding winter, but a more pronounced reduction was observed following the February 2025 frost event,

consistent with cold-induced photoinhibition [20]. Cultivar differences were evident during the post-frost period, with ‘Gem’ exhibiting the highest Fv/Fm values in April 2025. By May, Fv/Fm values had recovered to approximately 0.82–0.85 in all cultivars, despite the pronounced differences among cultivars in flowering and subsequent yield. This divergence indicates that recovery of maximum PSII efficiency did not necessarily parallel reproductive recovery following frost. The absence of a significant overall cultivar effect, together with the significant cultivar × sampling date interaction (Table 3), indicates that these differences were date-specific rather than consistent throughout the study.

Leaf chlorophyll is commonly associated with plant physiological status, photosynthetic capacity, and dry matter production [36]. Although ‘BL’ frequently exhibited relatively high CCI values at specific sampling dates (Fig. 6), the absence of a significant overall cultivar effect, together with the significant cultivar × sampling date interaction (Table 3), indicates that cultivar differences were not consistent throughout the study. A similar tendency toward relatively high CCI in ‘BL’ was previously observed in young trees [22]. Other studies have shown that cold stress can reduce CCI in ‘Hass’ and in the evergreen tree *Quercus ilex* [21, 37]. Despite its relatively high CCI on many sampling dates, ‘BL’ sustained extensive floral bud damage in 2025 and produced a very low yield after the frost event (Figs. 3, 4). Thus, the performance of ‘BL’ suggests that maintaining high leaf chlorophyll content alone is not sufficient to ensure reproductive resilience under severe frost conditions.

In addition to the winter frost event, the experimental orchard experienced episodes of exceptionally high summer air temperature, with a maximum of 47.2°C (Fig. 2). Gas-exchange rates were lower on some summer sampling dates (Fig. 5); however, because measurements were not designed as event-specific pre- and post-heat comparisons, the contribution of heat stress cannot be separated from other seasonal factors. Accordingly, the summer observations should be interpreted as physiological responses under naturally occurring high-temperature field conditions rather than as a direct test of cultivar heat tolerance. Unlike the response following frost, no comparable decline in Fv/Fm or obvious visible foliar damage was observed during the hottest periods (Fig. 6). This is consistent with previous findings in mature ‘Pinkerton’ avocado trees, where extreme heat conditions did not result in visible foliar damage [6]. Although ‘Gem’ maintained relatively high CO_2 assimilation and g_s on some summer sampling dates, these date-specific differences do not establish greater intrinsic heat tolerance.

The PCA provided an integrated view of cultivar performance but was interpreted as an exploratory summary of trait covariation rather than as evidence of distinct cultivar strategies (Supplementary Fig. 2). Yield and fruit number were closely associated, whereas mean fruit weight loaded in the opposite direction. Given the inherent mathematical relationship among these variables, this pattern was interpreted descriptively rather than as evidence of a physiological tradeoff. Gas-exchange variables were closely aligned, indicating that CO_2 assimilation and g_s varied together across cultivars and seasons. ‘BL’ was associated with higher gas exchange, CCI, and fruit weight, whereas ‘Hass’ associated more strongly with yield and fruit number. ‘Maluma’ tended to occupy a region of the ordination associated with lower reproductive output. ‘Gem’ occupied an intermediate position, indicating an intermediate multivariate trait profile rather than consistent superiority in any single group of traits.

Overall, the PCA complements the trait-specific mixed-model analyses by visualizing covariation among physiological and productivity variables, but it does not provide independent evidence for causal relationships among these traits.

Several limitations define the scope of inference from this study. The experiment was conducted at a single site and included one major frost event, and cultivar-specific floral bud phenology at the time of freezing was not quantified. Previous-season crop load also differed among cultivars and may have contributed to subsequent yield responses. In addition, the summer heat component was observational rather than an event-specific stress experiment. Therefore, the present results should be interpreted as evidence of cultivar-dependent field responses under the conditions studied, rather than as proof of intrinsic frost or heat tolerance.

A major contribution of this study is the integration of repeated physiological measurements with reproductive injury, flowering, fruit number, and yield in mature avocado cultivars under naturally occurring field conditions. Previous field studies in avocado have examined the physiological responses of mature trees to winter protection or extreme heat, but have generally focused on a single cultivar and therefore have not addressed whether cultivar-dependent stress responses are accompanied by differences in subsequent reproductive performance [6, 13]. In contrast to previous work in young, non-bearing ‘Hass’ and ‘Hass’-like trees, the present study links cultivar-dependent responses to weather extremes with subsequent reproductive performance and yield in mature, fruit-bearing trees [22]. This distinction is particularly important because recovery of leaf-level physiological indicators did not necessarily parallel reproductive recovery following frost. From an applied perspective, the significant cultivar × season and cultivar × sampling date interactions (Tables 2, 3) further indicate that cultivar performance should be evaluated across contrasting seasons and environmental conditions rather than on the basis of a single season or sampling date. Cultivar selection may therefore complement orchard-management practices designed to mitigate damage from temperature extremes [18, 21, 38, 39].

5. Conclusions

This three-year field study demonstrates substantial cultivar-dependent variation in the physiological and reproductive responses of mature, fruit-bearing avocado trees under Mediterranean weather extremes. The clearest contrast followed the severe February 2025 frost, when ‘Gem’ sustained lower floral bud injury and showed substantially greater post-frost flowering intensity and yield than ‘Hass’, ‘BL’, and ‘Maluma’. In contrast, Fv/Fm recovered to similar values in all cultivars within several months, and the relatively high CCI frequently observed in ‘BL’ was not accompanied by greater post-frost reproductive performance. These findings indicate that recovery or maintenance of individual leaf-level physiological traits does not necessarily parallel reproductive resilience at the whole-tree level. Under the conditions examined, ‘Gem’ showed the greatest reproductive resilience to the 2025 frost event, but additional multi-site and multi-event studies are required to determine the generality and underlying mechanisms of these cultivar-dependent responses.

Declarations

Ethics approval and consent to participate-

not applicable.

Consent for publication-

not applicable.

Competing interests-

The authors declare that they have no known competing financial interests or personal relationships that could have appeared to influence the work reported in this paper.

Funding-

This work was supported by the Israeli Fruit Board.

Author Contribution

Conceptualization, L.R., M.N. and N.S.; Investigation, M.L.; Formal analysis, L.R.; Writing-original draft preparation, M.L., M.N., N.S. and L.R.; Writing review and editing, M.L., M.N., N.S. and L.R.; Funding acquisition, L.R. All authors have read and agreed to the published version of the manuscript.

Acknowledgements-

The authors thank the ‘Mataim’ experimental farm team and Marc Perel for the effort that they invested in this study.

Data Availability

The datasets generated and/or analyzed during the current study are available from the corresponding author on reasonable request.

References

1. Alcaraz ML, Thorp TG, Hormaza JI. Phenological growth stages of avocado *(Persea americana)* according to the BBCH scale. Sci Hortic. 2013;164:434–9. https://doi.org/10.1016/j.scienta.2013.09.051.

2. Charrier G, Ngao J, Saudreau M, Améglio T. Effects of environmental factors and management practices on microclimate, winter physiology, and frost resistance in trees. Front Plant Sci. 2015;6 April:1–18. https://doi.org/10.3389/fpls.2015.00259.
3. Sidharthan B, Loganathan S, Sardar DS, Kujur AN, Kumar KMA, Deshpande HH, et al. Climate Change Impacts on Fruit Crop Productivity, Quality and Postharvest Performance: A Critical Review. Archives of Current Research International. 2026;26:541–61. https://doi.org/10.9734/acri/2026/v26i61980.
4. Sharma S, Manjeet M. Heat stress effects in fruit crops. Agricultural Reviews. 2020;41:73–8. https://doi.org/10.18805/ag.r-1951.
5. Shapira O, Chernoivanov S, Neuberger I, Levy S, Rubinovich L. Physiological characterization of young 'Hass' avocado plant leaves following exposure to high temperatures and low light intensity. Plants. 2021;10:1562. https://doi.org/10.3390/PLANTS10081562.
6. Alon E, Shapira O, Azoulay-Shemer T, Rubinovich L. Shading nets reduce canopy temperature and improve photosynthetic performance in 'Pinkerton' avocado trees during extreme heat events. Agronomy. 2022;12:1360. https://doi.org/10.3390/agronomy12061360.
7. Teskey R, Wertin T, Bauweraerts I, Ameye M, McGuire MA, Steppe K. Responses of tree species to heat waves and extreme heat events. Plant Cell Environ. 2015;38:1699–712. https://doi.org/10.1111/pce.12417.
8. Filewod B, Thomas SC. Impacts of a spring heat wave on canopy processes in a northern hardwood forest. Glob Chang Biol. 2014;20:360–71. https://doi.org/10.1111/GCB.12354.
9. Jouyban Z, Hasanzade R, Sharafi S. Chilling stress in plants. International Journal of Agriculture and Crop Sciences. 2013;5:2961–8.
10. Perry KB. Basics of frost and freeze protection for horticultural crops. Horttechnology. 1998;8:10–5. https://doi.org/10.21273/HORTTECH.8.1.10.
11. Whiley AW, Searle C, Schaffer B, Wolstenholme BN. Cool orchard temperatures or growing trees in containers can inhibit leaf gas exchange of avocado and mango. Journal of the American Society for Horticultural Science. 1999;124:46–51. https://doi.org/10.21273/jashs.124.1.46.
12. Chernoivanov S, Neuberger I, Levy S, Szenes N, Rubinovich L. Covering young 'Reed' avocado trees with shading nets during winter alleviates cold stress and promotes vegetative growth. Eur J Hortic Sci. 2022;87:1–10. https://doi.org/10.17660/eJHS.2022/007.
13. Rubinovich L, Sofer-Arad C, Chernoivanov S, Szenes N. Effects of Covering Mature Avocado 'Pinkerton' Trees with High-density Shading Nets during Cold Winters on Microclimate, Chlorophyll Fluorescence, Flowering, and Yield. HortScience. 2023;58:1201–4. https://doi.org/10.21273/HORTSCI17337-23.
14. Jones HG. Frost protection: fundamentals, practice, and economics. Volume 1. Exp Agric. 2006;42:369. https://doi.org/10.1017/S0014479706273794.
15. Verslues PE, Agarwal M, Katiyar-Agarwal S, Zhu J, Zhu JK. Methods and concepts in quantifying resistance to drought, salt and freezing, abiotic stresses that affect plant water status. Plant Journal. 2006;45:523–39. https://doi.org/10.1111/j.1365-313X.2005.02593.x.

16. De Melo-Abreu JP, Villalobos FJ, Mateos L. Frost protection. In: Villalobos FJ, Fereres E, editors. Principles of Agronomy for Sustainable Agriculture. Cham: Springer International Publishing; 2016. p. 443–57. https://doi.org/10.1007/978-3-319-46116-8_29.
17. Janda T, Szalai G, Rios-Gonzalez K, Veisz O, Páldi E. Comparative study of frost tolerance and antioxidant activity in cereals. Plant Science. 2003;164:301–6. https://doi.org/10.1016/S0168-9452(02)00414-4.
18. Bar-Noy Y, Sofer-Arad C, Perel M, Cohen H, Senesh N, Noy M, et al. Frost protection efficiency evaluation in avocado with a horizontal wind machine. Fruits. 2019;74:124–9. https://doi.org/10.17660/th2019/74.3.4.
19. Weil A, Sofer-Arad C, Bar-Noy Y, Liran O, Rubinovich L. Comparative study of leaf antioxidant activity as a possible mechanism for frost tolerance in 'Hass' and 'Ettinger' avocado cultivars. J Agric Sci. 2019;157:342–9. https://doi.org/10.1017/S0021859619000662.
20. Joshi NC, Yadav D, Ratner K, Kamara I, Aviv-Sharon E, Irihimovitch V, et al. Sodium hydrosulfide priming improves the response of photosynthesis to overnight frost and day high light in avocado (*Persea americana* Mill, cv. 'Hass'). Physiol Plant. 2019;168:394–405. https://doi.org/10.1111/ppl.13023.
21. Lahak M, Alon E, Chen A, Rubinovich L. Covering young avocado 'Hass' trees with high-density shading nets during the winter mitigates frost damage and improves tree performance. Trees. 2024;38:327–38. https://doi.org/10.1007/s00468-023-02485-3.
22. Lahack M, Noy M, Szenes N, Rubinovich L. Vegetative Growth, Flowering, and Physiological Parameters of Young Avocado "Hass" and 'Hass'-Like Cultivars Under Extreme Weather Conditions. International Journal of Fruit Science. 2025;25:378–92. https://doi.org/10.1080/15538362.2025.2561582.
23. Silva TA, Ledesma N. Avocado history, biodiversity and production. In: Nandawani D, editor. Sustainable Horticultural Systems. Springer International Publishing, Switzerland; 2014. p. 157–205. https://doi.org/10.1007/978-3-319-06904-3.
24. Arpaia ML, Smith H. Enhancement of avocado productivity. Plant improvement-selection and evaluation of improved varieties and rootstocks. In: Proceedings of the California avocado research symposium. Riverside, California: University of California and California Avocado Commission; 2004. p. 9–23.
25. Camiletti BX, Asensio CM, Carraro TA, Gusella G, Focht ED, Pandey R, et al. Influence of fruit maturity and variety on seasonal postharvest fungal diseases and vascular streaking in California Avocados. PLoS One. 2026;21:e0351752. https://doi.org/10.1371/journal.pone.0351752.
26. Ernst A. Maluma Hass®: A new released cultivar in comparison with Hass. In: Proceedings VI World Avocado Congress. 2007.
27. Witney G, Martin G. Taking the California avocado breeding program into the next century. In: Proceedings of The World Avocado Congress III. 1995. p. 114–8.

28. Micheletti LB, Avilés TC, Baptista EG, Alberti MF, Nacata G, do Amaral Brogio B, et al. Initial performance of “Gem” avocado trees in the Central-Western region of São Paulo State. Semina:Ciencias Agrarias. 2021;42:3123–34. https://doi.org/10.5433/1679-0359.2021v42n6p3123.
29. Schreiber U, Schliwa U, Bilger W. Continuous recording of photochemical and non-photochemical chlorophyll fluorescence quenching with a new type of modulation fluorometer. Photosynth Res. 1986;10:51–62. https://doi.org/10.1007/BF00024185.
30. Kramer DM, Johnson G, Kiirats O, Edwards GE. New fluorescence parameters for the determination of QA redox state and excitation energy fluxes. Photosynth Res. 2004;79:209–18. https://doi.org/10.1023/B:PRES.0000015391.99477.0d.
31. Baker NR. Chlorophyll fluorescence: a probe of photosynthesis *in vivo*. Annu Rev Plant Biol. 2008;59:89–113. https://doi.org/10.1146/annurev.arplant.59.032607.092759.
32. Ziv D, Zviran T, Zezak O, Samach A, Irihimovitch V. Expression profiling of *FLOWERING LOCUS T-like* gene in alternate bearing ‘Hass’ avocado trees suggests a role for *PaFT* in avocado flower induction. PLoS One. 2014;9:1–14. https://doi.org/10.1371/journal.pone.0110613.
33. Chung SW, Rho H, Lim CK, Jeon MK, Kim S, Jang YJ, et al. Photosynthetic response and antioxidative activity of ‘Hass’ avocado cultivar treated with short-term low temperature. Sci Rep. 2022;12:11593. https://doi.org/10.1038/s41598-022-15821-3.
34. Valdebenito S, Escobar M, Cautín R, Vidal J, Ruiz M, Astudillo B, et al. Comparison of Polyphenol Content and Antioxidant Activity in Leaves of Seven Avocado (*Persea americana* Mill.) Cultivars. Agronomy. 2026;16. https://doi.org/10.3390/agronomy16090929.
35. Zait Y, Elingold I, Londener A, Gal E, Or G, Galpaz N. Banana frost protection by thermal nets. In: Acta Horticulturae. Istanbul, Turkey: International Society for Horticultural Science; 2020. p. 21–6. https://doi.org/10.17660/ActaHortic.2020.1272.3.
36. Croft H, Chen JM, Wang R, Mo G, Luo S, Luo X, et al. The global distribution of leaf chlorophyll content. Remote Sens Environ. 2020;236 November 2019. https://doi.org/10.1016/j.rse.2019.111479.
37. Oliveira G, Peñuelas J. Comparative photochemical and phenomorphological responses to winter stress of an evergreen (*Quercus ilex* L.) and a semi-deciduous (*Cistus albidus* L.) Mediterranean woody species. Acta Oecologica. 2000;21:97–107. https://doi.org/10.1016/S1146-609X(00)00121-1.
38. Dag A, Vitoshkin H, Resef G, Ron Y, Alchanatis V. Evaluating Overhead Sprinklers and Sprayers for Heatwave Protection in Avocado Orchards. Plants. 2026;15:1516. https://doi.org/10.3390/plants15101516.
39. El-Moniem EAAA, Yousef ARM, Mahmoud TSM, Emam OA, Rohim FM, El-lethy SR. Potassium and Aluminum Silicate Application to Alleviate the Adverse Effects of Heat Stress on ‘Hass’ and ‘Red’ Avocado Trees. Applied Fruit Science. 2026;68. https://doi.org/10.1007/s10341-025-01727-7.

Figures



Figure 1

Experimental site in northern Israel.

Aerial view of the experimental avocado orchard showing the spatial distribution of the four cultivars. Highlighted tree canopies represent ‘Hass’ (black), ‘BL’ (light green), ‘Gem’ (blue), and ‘Maluma’ (red). Each cultivar comprised five replicate plots, with three adjacent trees per replicate. ‘Ettinger’ (yellow) trees were planted as pollinizers, comprising 11% of the plot.

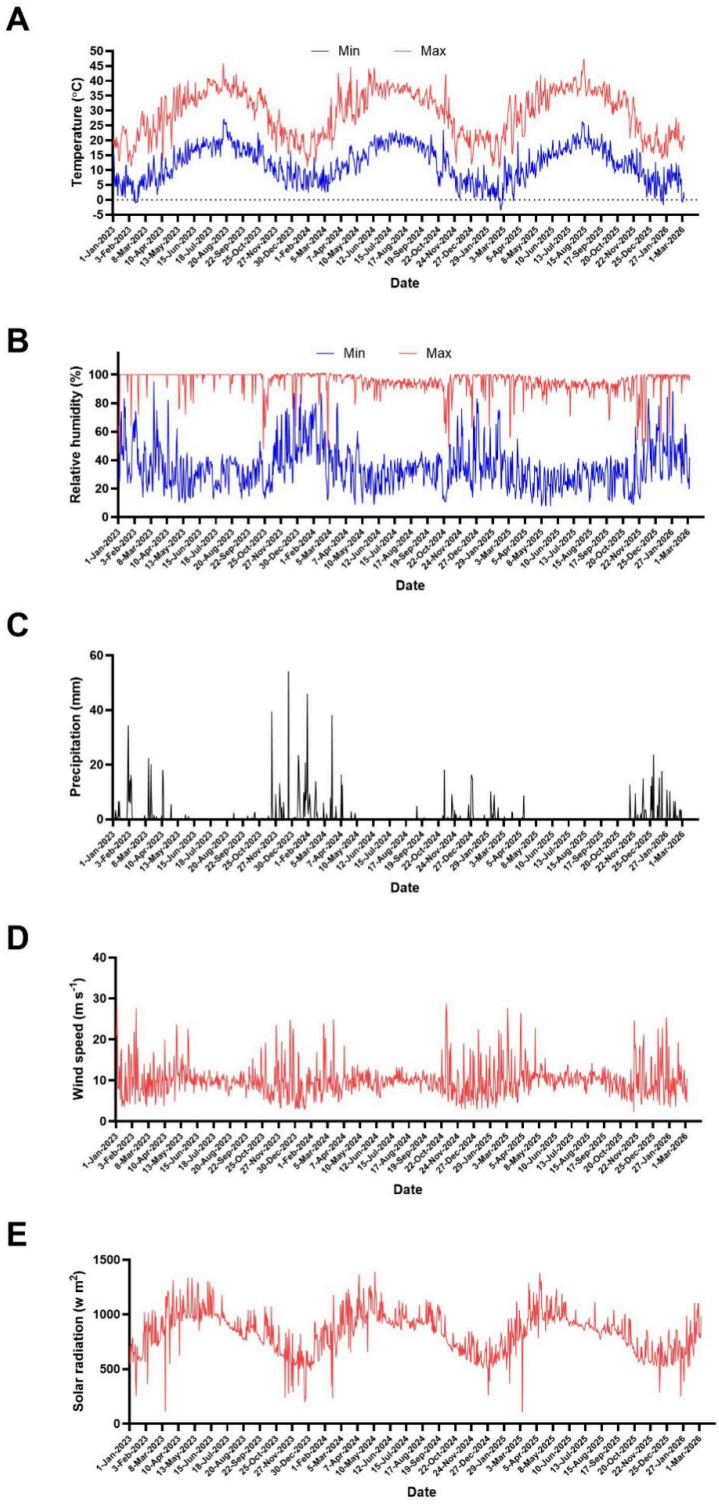


Figure 2

Meteorological data. (A) Minimum and maximum daily air temperature. (B) Minimum and maximum daily relative humidity. (C) Precipitation. (D) Maximum daily wind speed. (E) Maximum daily solar radiation. Data were recorded from January 2023 to March 2026 at ‘Ha-Hula’ weather station, close to the experimental site.

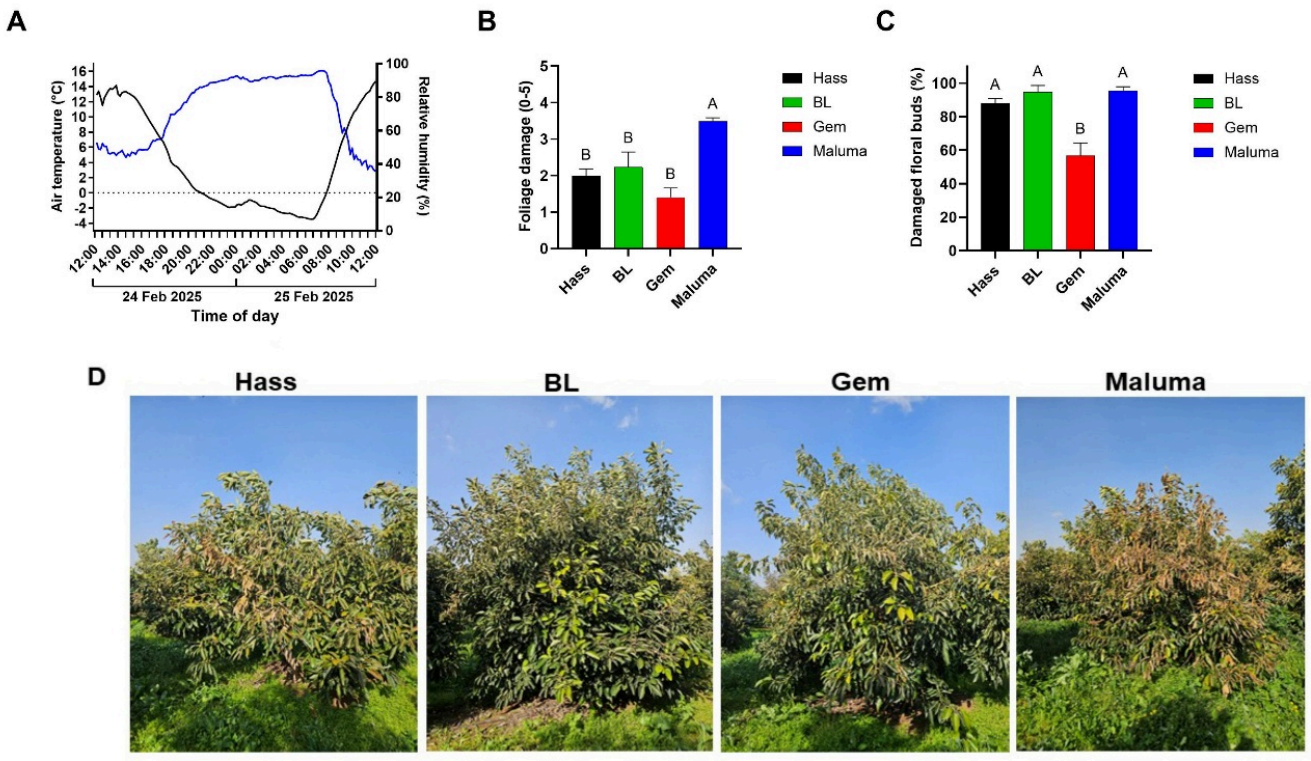


Figure 3

Damage to foliage and floral buds following the severe frost event in February 2025. (A) Daily air temperature (black) and relative humidity (blue), recorded at 10-min intervals in the experimental plot on 24 and 25 Feb 2025 (data are the mean of two data loggers). (B) Damage to foliage and (C) floral buds in the experimental trees at the beginning of March 2025. Values are means ± SE of five replicate plots (n = 5, three trees per replicate). Different letters indicate significant differences among cultivars ($P < 0.05$). Foliage damage was analyzed by one-way ANOVA followed by Tukey's HSD test, and floral bud damage by binomial GLMM with Tukey–Kramer-adjusted pairwise comparisons. (D) Representative photos of the experimental trees. Pictures were taken in March 2025.

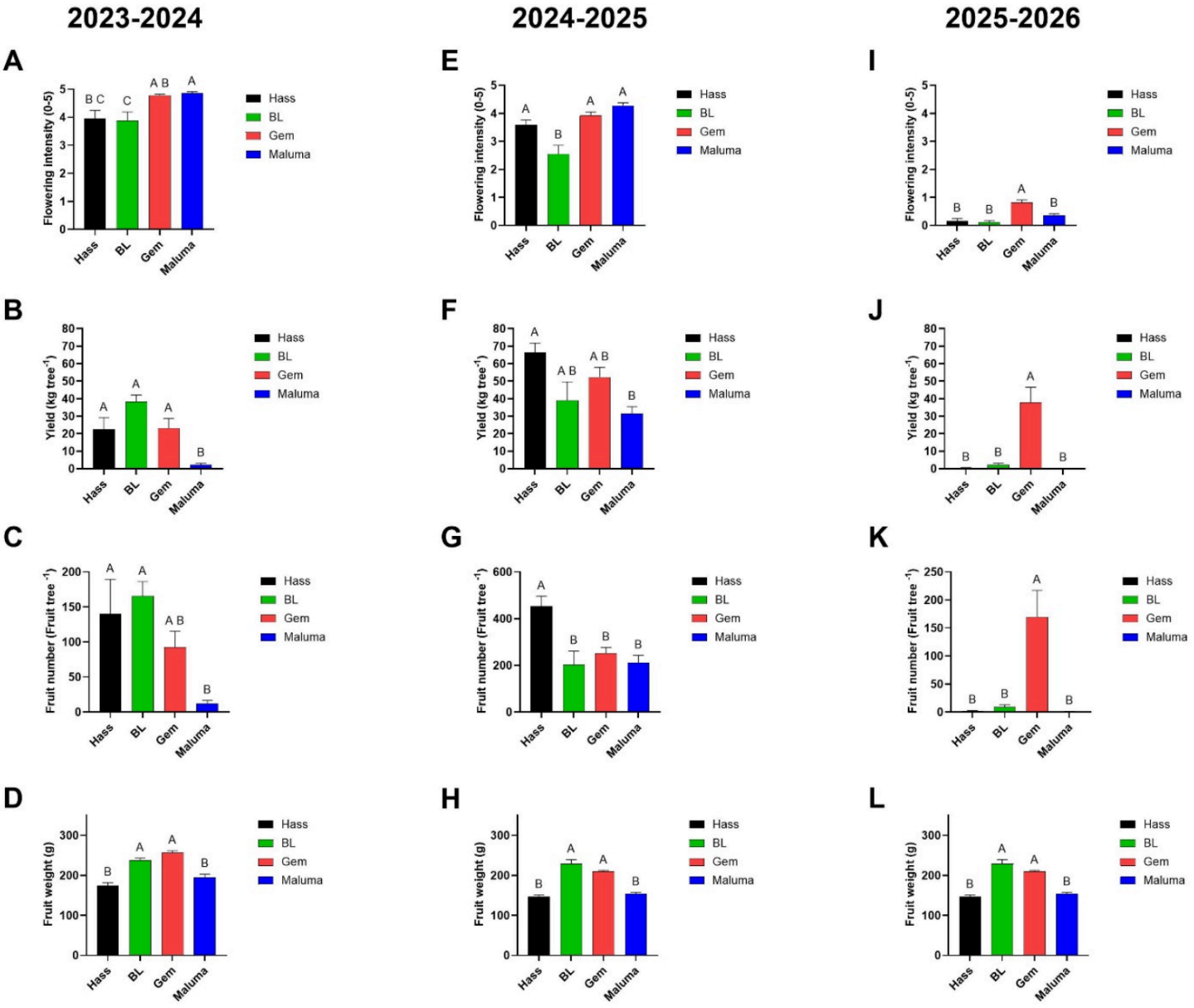


Figure 4

Flowering intensity and productivity traits of the experimental avocado cultivars.

Flowering intensity was assessed and scored in (A) April 2023, (E) April 2024, and (I) April 2025 on a scale of 0–5, with 0 representing no apparent flowering and 5, maximum bloom. (B, F, J) Fruit yield and (C, G, K) number of fruits per tree were determined on the commercial harvest date of each cultivar in the growing seasons of 2023–2024 (B, C), 2024–2025 (F, G), and 2025–2026 (J, K). (D, H, L) Mean fruit weight for the three respective seasons was calculated for the same harvest period by dividing the total fruit weight by the number of fruits on each tree. Values are means ± SE of five replicate plots (n = 5, three trees per replicate). Different letters above a column indicate significant differences within each growing season (Tukey-adjusted comparisons, $P < 0.05$).

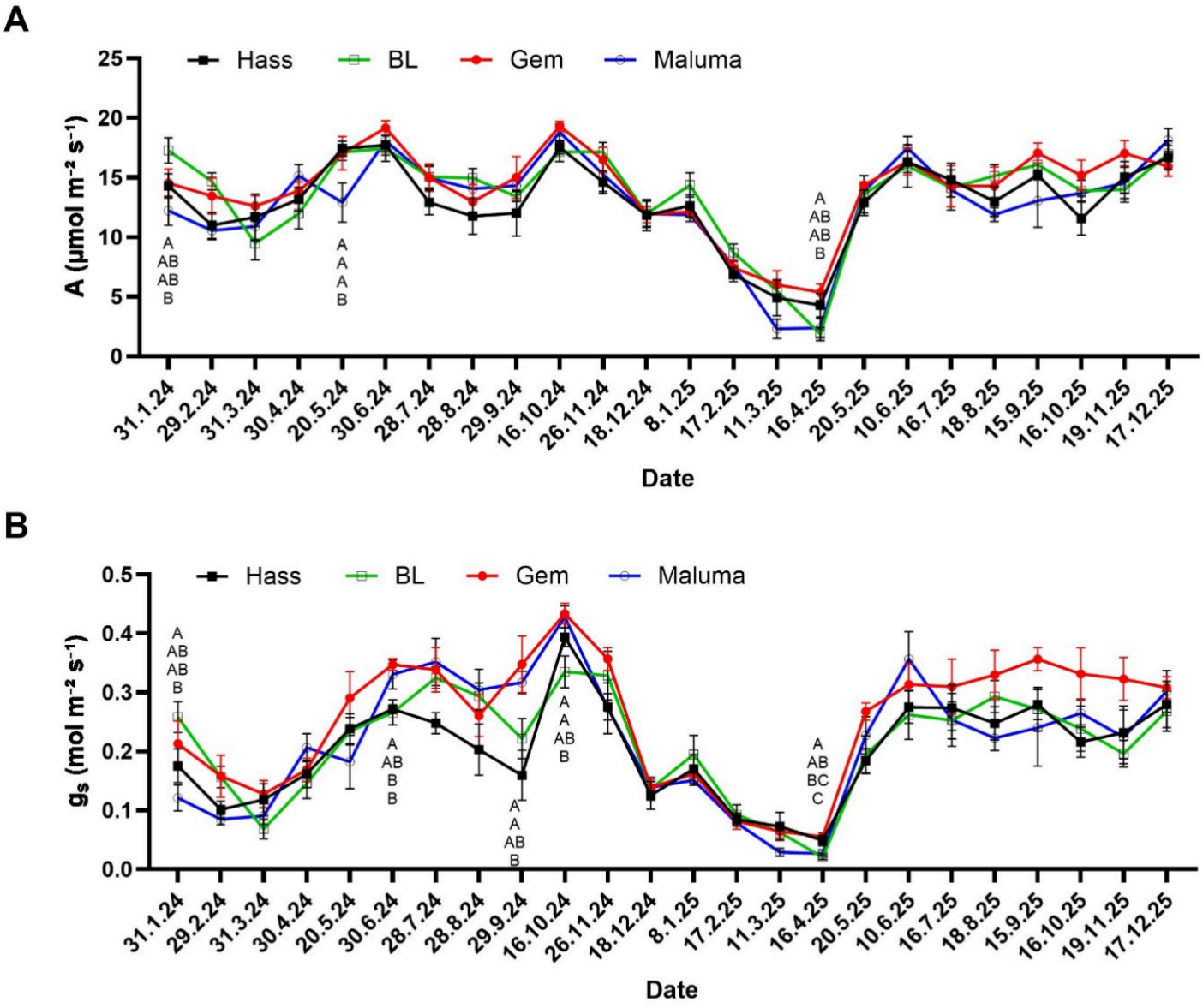


Figure 5

Leaf-level gas-exchange parameters.

The LI-COR system was used to measure and calculate (A) net CO_2-assimilation rate (defined as A) and (B) stomatal conductance to water vapor (g_s). Parameters were measured in the orchard periodically at mid-day from January 2024 to December 2025. Values are means ± SE of five replicate plots (n = 5; one tree per replicate; three different leaves were measured from each tree). Different letters indicate significant differences on the specified date (Tukey-adjusted comparisons, $P < 0.05$). Dates are given as day.month.year.

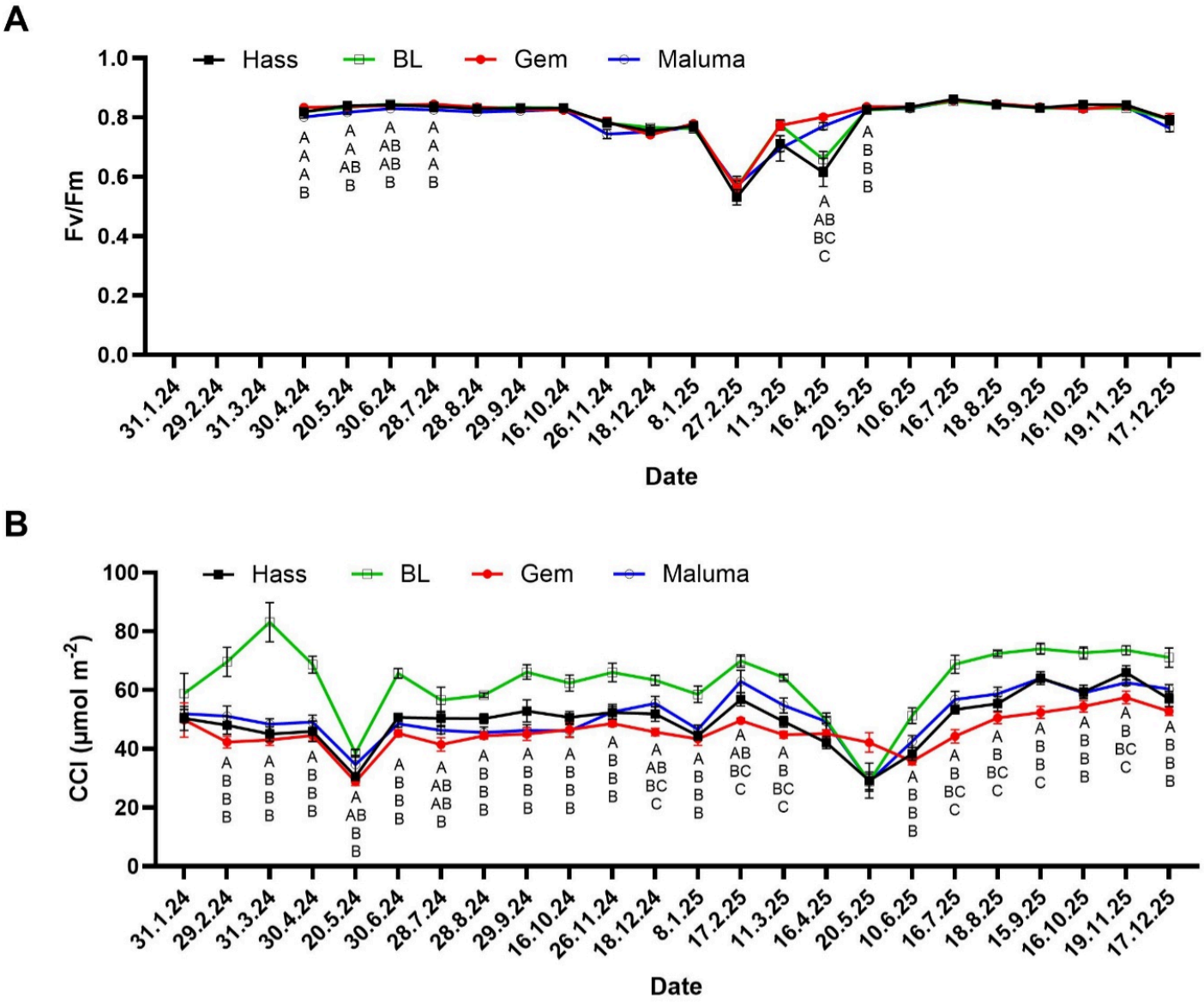


Figure 6

(A) Maximum quantum yield (Fv/Fm) and (B) leaf chlorophyll content (CCI).

Chlorophyll *a* fluorescence was recorded after dark adaptation to calculate Fv/Fm. Parameters were measured in the orchard periodically from January 2024 to December 2025. Fv/Fm was measured in the dark at night. Values are means ± SE of five replicate plots (n = 5, three trees per replicate; three different leaves were measured from each tree). Different letters indicate significant differences on the specified date (Tukey-adjusted comparisons, $P < 0.05$). Dates are given as day.month.year.

Supplementary Files

This is a list of supplementary files associated with this preprint. Click to download.

- floatimage7.jpeg
- floatimage8.jpeg